Estimation of fracture parameters from reflection seismic data, Part III: Fractured models with monoclinic symmetry

Andrey Bakulin*, Vladimir Grechka†, and Ilya Tsvankin†

*Schlumberger Cambridge Research, High Cross, Madingley Road, Cambridge, CB3 0EL, England
(Previous address: Department of Geophysics, St.-Petersburg State University, St. Petersburg, Russia)
† Center for Wave Phenomena

ABSTRACT

Aligned vertical cracks in otherwise isotropic background rock lead to anisotropy of the resulting medium. We use the linear slip theory developed by Schoenberg to obtain the effective parameters of monoclinic media due to the presence of (i) two different non-orthogonal sets of rotationally invariant fractures or (ii) one set of rotationally non-invariant, micro-corrugated fractures in an isotropic host rock.

The relationship between the anisotropic coefficients of the effective medium and parameters of two non-orthogonal sets of cracks shows that not only the orientations of fractures but also their compliances govern both the polarization directions of the vertically propagating split shear waves and azimuthal variations of the normal-moveout (NMO) velocities of pure modes reflected from a horizontal interface. While the S-wave polarization azimuths are determined by the fracture orientations and tangential compliances, the directions of the semi-axes of the P-wave NMO ellipse also depend on normal compliances. We prove the possibility of complete fracture-characterization procedure (i.e., obtaining the velocities in isotropic host, compliances and orientations of two fracture systems) using the vertical velocities of P- and two split S-waves, and their NMO ellipses from a horizontal reflector.

One set of aligned vertical fractures with micro-corrugated surfaces also produces an effective monoclinic medium. In this case, monoclinic symmetry is entirely due to the coupling between the normal and tangential (to fracture faces) slips caused by micro-corrugation. The shear-wave splitting coefficient $\gamma^{(S)}$ in media with such microstructure, contrary to existing understanding, may depend on the *fluid content* of the fractures. We show that, in accordance with some recent experimental observations, the values of $\gamma^{(S)}$ for dry cracks are always greater than those for fluid-filled ones.

Key words: multiple fracture sets, monoclinic effective media, parameter estimation, infill-dependent shear-wave splitting

Introduction

Characterization of naturally fractured reservoirs using seismic data has been an area of active research over the past decade. Although various seismic signatures of P-, or S-, or converted PS-waves have proved to be useful in estimating parameters of fractures, current methods are designed to infer mainly qualitative information about fractures from seismic data. A review of recent publications related to fracture characterization can be found in Bakulin et al. (1999a; 1999b) which hereinafter will be referred to as Paper I and Paper II.

Theoretical tools (the so-called effective media theories) for solving the fracture-characterization problem exist since the early 1980s (Schoenberg, 1980; 1983; Hud-

son, 1980; 1981; 1988; Thomsen, 1995). The general treatment of fractures as highly compliant surfaces inside a solid host rock, known as the linear slip theory, was developed by Schoenberg (1980, 1983) and Schoenberg and Muir (1989). According to this theory, the effective compliance of a rock with fractures can be found as the sum of the compliances of the host rock and all fractures. Therefore, the effective elastic stiffness coefficients become functions of the stiffnesses of the host rock and fracture compliances, which are the inherent parameters of the linear slip theory. This, in principle, allows one to relate the effective Thomsen-type anisotropic coefficients, which govern the influence of anisotropy on various seismic signatures, to the fracture compliances, and ultimately recover the compliances from seismic data*. We followed this idea in Paper I where we discussed which seismic signatures can be used to estimate the compliances and orientation of a single set of vertical rotationally-invariant fractures embedded in an isotropic host rock which produce the simplest effective model of fractured media – transverse isotropy with a horizontal symmetry axis (HTI). We extended our approach to orthorhombic media due to one system of vertical fractures in a VTI (transversely isotropic with a vertical symmetry axis) background and to two orthogonal fracture sets in a purely isotropic host rock (Paper II). Here, we examine more complicated fractured media with monoclinic symmetry.

We discuss two types of fracture systems. The first model contains two different non-orthogonal sets of rotationally invariant cracks in an isotropic background. The corresponding effective medium is monoclinic with a horizontal symmetry plane. We prove that all fracture parameters – the compliances normal and tangential to the crack faces, and the azimuths of both fracture sets – can be estimated given the vertical and NMO velocities (from a horizontal reflector) of the P- and two split S-waves. Also, we confirm the conclusion of Grechka et al. (1999) that the polarization directions of vertically propagating shear-waves are generally *different* from the directions of semi-axes of P-wave NMO ellipses (which cannot happen in the higher-symmetry transversely isotropic or orthorhombic media). A similar conclusion was made by Sayers (1998) who examined the azimuthal variation of the P-wave phase-velocity function. Those results gives possible theoretical explanation of discrepancies in fracture orientation estimated from P- and S-wave data observed by Perez et al. (1999).

The second model consists of a single set of micro-corrugated (rotationally non-invariant) fractures in isotropic host rock. The effective medium in this case is monoclinic with a vertical symmetry plane. We show that the coupling between the normal and tangential to crack faces slips, caused by micro-corrugation, produces shear-wave splitting which may depend on the *fluid content* of the fractures. Such a possibility, to the best of our knowledge, has not been examined so far [Schoenberg and Douma (1988), and Berg et al. (1991) are the only references where the coupling between normal and tangential compliances is discussed]. Although it is conventionally believed that shear-wave splitting depends only on the crack density, recent observations of Guest et al. (1998) may support our model.

Two sets of vertical fractures

Effective parameters of rocks with two systems of cracks

Effective compliance $\mathbf{s}$ of a rock with multiple fracture sets can be represented as the sum of the compliance $\mathbf{s}_b$ of background medium and the fracture compliances $\mathbf{s}_f$ (Schoenberg and Muir, 1989; Nichols et al., 1989; Molotkov and Bakulin, 1997; Bakulin and Molotkov, 1998). Here, we consider two different arbitrarily oriented sets of vertical, rotationally invariant fractures (with compliances $\mathbf{s}_{f1}$ and $\mathbf{s}_{f2}$) in isotropic host rock, so that the effective compliance is given by

$$\mathbf{s} = \mathbf{s}_b + \mathbf{s}_{f1} + \mathbf{s}_{f2} \equiv \mathbf{c}^{-1}, \tag{1}$$

where $\mathbf{c}$ is the stiffness matrix of effective medium. The compliance $\mathbf{s}_b$ of the isotropic background, written in terms of the Lamé parameters λ and μ, has the form:

$$\mathbf{s}_b = \begin{pmatrix} \frac{\lambda+\mu}{\mu\ell} & -\frac{\lambda}{2\mu\ell} & -\frac{\lambda}{2\mu\ell} & 0 & 0 & 0 \\ -\frac{\lambda}{2\mu\ell} & \frac{\lambda+\mu}{\mu\ell} & -\frac{\lambda}{2\mu\ell} & 0 & 0 & 0 \\ -\frac{\lambda}{2\mu\ell} & -\frac{\lambda}{2\mu\ell} & \frac{\lambda+\mu}{\mu\ell} & 0 & 0 & 0 \\ 0 & 0 & 0 & \frac{1}{\mu} & 0 & 0 \\ 0 & 0 & 0 & 0 & \frac{1}{\mu} & 0 \\ 0 & 0 & 0 & 0 & 0 & \frac{1}{\mu} \end{pmatrix}, \tag{2}$$

where $\ell = 3\lambda + 2\mu$.

The compliance matrices $\mathbf{s}_{fi}$ $(i = 1, 2)$ of each rotationally invariant fracture set are described by the normal and tangential to crack faces compliances, K_{Ni} and K_{Ti}, respectively. These matrices have the simplest form when the normals $\mathbf{n}_i$ to the ith fracture sets point in the direction of either x_1 or x_2 coordinate axes. Choosing,

* Schoenberg and Douma (1988), as well as Paper I, show that fracture compliances effectively absorb such information about microstructure of fractures as the shape of cracks, their possible interaction, partial saturation, the presence or absence of equant porosity, etc. This information cannot be obtained unambiguously from seismic data unless we make certain assumptions about fracture microstructure and microgeometry.

for definiteness, axis x_1 yields (Schoenberg and Douma, 1988; Schoenberg and Sayers, 1995; Paper I):

$$\mathbf{s}_{fi}^{x_1} = \begin{pmatrix} K_{Ni} & 0 & 0 & 0 & 0 & 0 \\ 0 & 0 & 0 & 0 & 0 & 0 \\ 0 & 0 & 0 & 0 & 0 & 0 \\ 0 & 0 & 0 & 0 & 0 & 0 \\ 0 & 0 & 0 & 0 & K_{Ti} & 0 \\ 0 & 0 & 0 & 0 & 0 & K_{Ti} \end{pmatrix} . \qquad (3)$$

Rotation of the fractures by the angle ϕ_i with respect to x_1-axis changes matrix (3) according to the so-called Bond transformation,

$$\mathbf{s}_{fi} = \mathbf{N}(\phi_i)\, \mathbf{s}_{fi}^{x_1}\, \mathbf{N}^{\mathbf{T}}(\phi_i)\,, \qquad (4)$$

where the 6×6 matrix $\mathbf{N}$ is explicitly written in Winterstein (1990), and $\mathbf{N}^{\mathbf{T}}$ is the transposed matrix. The exact expressions for elements of matrix $\mathbf{s}_{fi}$, obtained by Schoenberg et al. (1999), are given in Appendix A.

Equations (1)–(4) allow one to calculate the compliance ($\mathbf{s}$) or the stiffness ($\mathbf{c}$) matrices of the effective medium resulting from the presence of two fracture sets in isotropic background. Analyzing equations (A1)–(A9) shows that such effective medium is monoclinic with a horizontal symmetry plane. Below, we show how to invert the anisotropic coefficients of the effective monoclinic medium for parameters of fractures.

Anisotropic coefficients of monoclinic media

Dimensionless anisotropic coefficients, first introduced by Thomsen (1986) for transversely isotropic media with a vertical axis of symmetry (VTI model), proved to be extremely useful in describing various seismic signatures. Since Thomsen's work, several generalizations of anisotropic coefficients to more complicated symmetries have been made. Rüger (1997) and Tsvankin (1997a) introduced Thomsen-style notation for transversely isotropic media with a horizontal symmetry axis (HTI model). Similar anisotropic coefficients for orthorhombic media, defined by Tsvankin (1997b), were shown to simplify azimuthally varying normal-moveout velocities or the NMO ellipses (Grechka and Tsvankin, 1998) of reflected waves. Grechka and Tsvankin (1999) found the subset of those coefficients which can be determined using P-wave surface reflection data.

Extending the Thomsen-type notation to monoclinic media, Grechka et al. (1999) noticed that anisotropic coefficients, which determine P- and S-wave NMO ellipses from horizontal reflectors, have the simplest form when the horizontal coordinate axes x_1 and x_2 coincide with the polarization directions of two vertically propagating split shear waves (S_1 and S_2). In this natural coordinate frame the stiffness coefficient c_{45} vanishes (Helbig, 1994; and Mensch and Rasolofosaon, 1997):

$$c_{45} = 0\,. \qquad (5)$$

Grechka et al. (1999) introduced the set of twelve anisotropic parameters: V_{P0}, V_{S0}, $\epsilon^{(1,2)}$, $\delta^{(1,2,3)}$, $\gamma^{(1,2)}$, and $\zeta^{(1,2,3)}$ (Appendix B). Those parameters fall into two distinctive groups. The first group contains the vertical velocities V_{P0}, V_{S0}, and the Thomsen-type ϵ-, δ-, and γ-coefficients which are defined in the same way as Tsvankin's (1997b) anisotropic parameters for the higher-symmetry orthorhombic media. These quantities mainly control the NMO velocities of pure modes in the polarization directions x_1 and x_2 of two vertically propagating shear waves. The second group consists of three ζ-coefficients which are responsible for the *rotations* of P, S_1, and S_2 NMO ellipses with respect to the coordinate axes (Grechka et al., 1999). The ζ-coefficients are defined in such a way [see equations (B10)–(B12)] that $\zeta^{(3)}$ describes the rotation of P-wave NMO ellipse while $\zeta^{(1)}$ and $\zeta^{(2)}$ govern the rotations of S_1- and S_2-ellipses respectively.

Grechka et al. (1999) showed that eleven out of twelve anisotropic parameters in monoclinic media can be estimated in a stable way using the vertical velocities of P- and two split S-waves and the NMO ellipses of pure modes reflected from a horizontal interface. The only coefficient which is not constrained by conventional-spread moveout data from horizontal reflectors is $\delta^{(3)}$.

Estimation of fracture parameters

Let us assume that the quantities V_{P0}, V_{S0}, $\epsilon^{(1,2)}$, $\delta^{(1,2)}$, $\gamma^{(1,2)}$, and $\zeta^{(1,2,3)}$ have already been obtained (see Grechka et al., 1999) and show that they provide sufficient information to estimate eight parameters characterizing fractures. The parameters to be found include P- and S-wave velocities V_P and V_S in the isotropic background, two azimuths ϕ_1 and ϕ_2 of the normals to the fracture faces, and four dimensionless weaknesses Δ_{Ni} and Δ_{Ti} which relate to the fracture compliances K_{Ni} and K_{Ti} as follows (Hsu and Schoenberg, 1993; Paper I)

$$\Delta_{Ni} = \frac{(\lambda + 2\mu)\, K_{Ni}}{1 + (\lambda + 2\mu)\, K_{Ni}}$$

and

$$\Delta_{Ti} = \frac{\mu\, K_{Ti}}{1 + \mu\, K_{Ti}}\,, \qquad (i = 1, 2)\,. \qquad (6)$$

The weaknesses Δ_{Ni} and Δ_{Ti} are always positive and vary from 0 to 1. If we ignore the influence of one system of fractures on another, which may be a reasonable assumption when both crack densities e_i are small, and consider isolated penny-shaped cracks, then vanishing values of the ratios Δ_{Ni}/Δ_{Ti} will correspond to fluid-filled fractures, whereas the ratios $\Delta_{Ni}/\Delta_{Ti} \approx (\lambda + 2\mu)/\mu$ (or $K_{Ni} \approx K_{Ti}$) indicate dry cracks. Also, in the absence of the second fracture system, the tan-

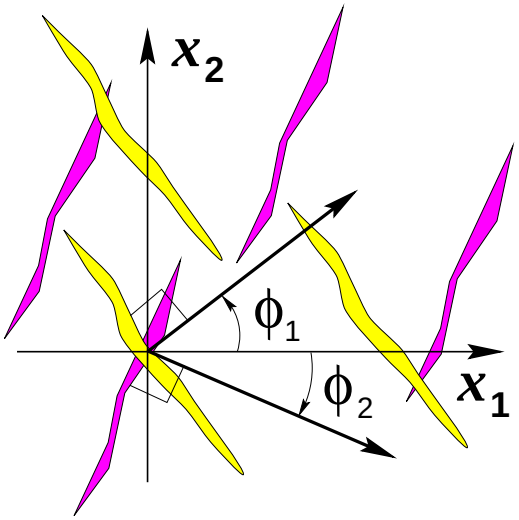

Figure 1. Two sets of vertical fractures oriented at azimuths ϕ_1 and ϕ_2 with respect to polarization direction x_1 of vertically propagating S_1-wave.

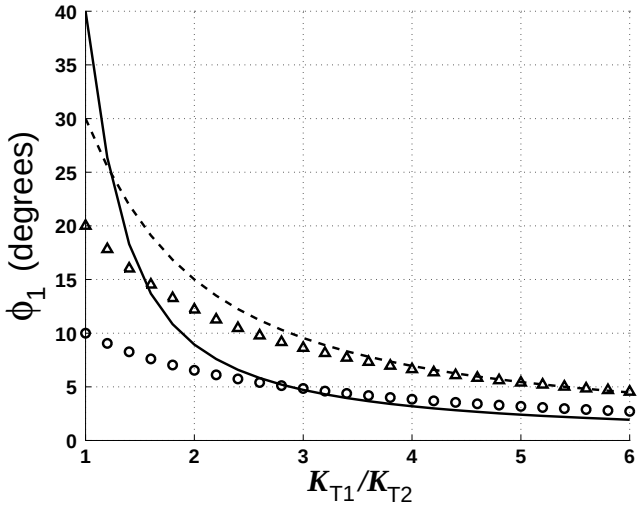

Figure 2. Azimuth ϕ_1 as a function of the ratio of the compliances K_{T1}/K_{T2}. The angle between the fracture systems $\phi_1 - \phi_2 = 20°$ (circles), 40° (triangles), 60° (dashed line), and 80° (solid line).

gential weaknesses Δ_{Ti} are approximately equal to the doubled crack densities e_i regardless the type of fracture infill (Paper I). We assume that this relation holds in the presence of two systems of fractures which, again, can be justified when $e_i \ll 1$.

To estimate the fracture parameters, we need to specify a certain direction in the horizontal plane with respect to which the azimuths ϕ_1 and ϕ_2 are going to be measured. We choose, for definiteness, the polarization direction x_1 of vertically propagating S_1-wave (Figure 1). Our coordinate frame is now coincides with that where the anisotropic coefficients of monoclinic media have been defined by Grechka et al. (1999). In this coordinate frame, c_{45} vanishes [equation (5)] providing an additional constraint for the fracture parameters.

This constraint can be obtained by analyzing the nonzero elements of the matrices $\mathbf{s}_b$ [equation (2)] and $\mathbf{s}_{f1}$, $\mathbf{s}_{f2}$ [equations (A1)–(A9)] which comprise the effective compliance $\mathbf{s}$ [equation (1)]. Clearly, s_{44}, s_{45}, and s_{55} are the only nonzero elements of the fourth and fifth columns and the fourth and fifth rows of matrix $\mathbf{s}$. Thus, the compliance matrix $\mathbf{s}$ can be inverted as a block matrix to produce the stiffness matrix $\mathbf{c} = \mathbf{s}^{-1}$. The matrix $\mathbf{c}$ has a block

$$\begin{pmatrix} c_{44} & c_{45} \\ c_{45} & c_{55} \end{pmatrix} = \begin{pmatrix} s_{44} & s_{45} \\ s_{45} & s_{55} \end{pmatrix}^{-1},$$

which immediately indicates that $c_{45} = 0$ requires

$$s_{45} = 0\,. \tag{7}$$

This condition can be satisfied only when [see equations (1), (2) and (A7)]

$$K_{T1} \sin 2\phi_1 + K_{T2} \sin 2\phi_2 = 0 \tag{8}$$

or, equivalently, when [equation (6)]

$$\frac{\Delta_{T1}}{1-\Delta_{T1}} \sin 2\phi_1 + \frac{\Delta_{T2}}{1-\Delta_{T2}} \sin 2\phi_2 = 0\,. \tag{9}$$

Thus, we have twelve constraints [equations for eleven anisotropic parameters V_{P0}, V_{S0}, $\epsilon^{(1,2)}$, $\delta^{(1,2)}$, $\gamma^{(1,2)}$, and $\zeta^{(1,2,3)}$, and condition (9)] for eight fracture parameters V_P, V_S, Δ_{Ni}, Δ_{Ti}, and ϕ_i ($i = 1, 2$). The relations between the anisotropic coefficients and fracture parameters are nonlinear so, in general, inversion can be done only numerically. We will show that it converges to values close to the correct solution given reasonable errors in anisotropic coefficients.

Analyzing equations (8) and (9), we can make two important conclusions about the fracture orientation even prior to the inversion. First, since both Δ_{T1} and Δ_{T2} are nonnegative, equation (9) shows that fracture azimuths ϕ_1 and ϕ_2 always have opposite signs (Figure 1). Therefore, the angle between the two crack systems is $\phi_1 - \phi_2$. The absolute values of azimuths ϕ_1 and ϕ_2 are equal if and only if $\Delta_{T1} = \Delta_{T2}$. Second, equation (8) indicates that the fracture azimuths ϕ_1 and ϕ_2 depend only on the ratio of the tangential compliances K_{T1}/K_{T2}. The shear-wave polarization direction bisects the angle between the fractures if the two systems have equal compliances, i.e., if $K_{T1} = K_{T2}$ (Figure 2). If one system of fractures has greater tangential compliance than the other, the polarization direction of S_1-wave rapidly moves toward the system with the larger compliance. For example, as shown in Figure 2, the angle ϕ_1 between the normal to the first system of fractures and the S_1-polarization direction does not exceed 10° if

	V_S/V_P	Δ_{N1}	Δ_{T1}	ϕ_1	Δ_{N2}	Δ_{T2}	ϕ_2
Correct	0.5	0.25	0.12	30°	0.00	0.20	−13°
Estimated	0.5	0.20	0.04	40°	0.08	0.22	−5°

Table 1. Comparison of the correct fracture parameters with those estimated using the linearized formulae from Appendix D.

$K_{T1}/K_{T2} > 3$ regardless of the angle between the two crack systems.

Weak anisotropy

If the fracture density is small so that the weaknesses $\Delta_{Ni} \ll 1$ and $\Delta_{Ti} \ll 1$, the anisotropy of the effective medium is weak, and it becomes possible to derive linearized expressions for anisotropic coefficients in terms of fracture parameters. Those expressions, fully linearized in Δ_{Ni} and Δ_{Ti}, are given in Appendix C. Analyzing equations (C1)–(C11), we see that all ϵ-, δ-, and γ-coefficients are symmetric functions of fracture azimuths ϕ_1 and ϕ_2 and do not allow us to find the signs of azimuths. Information about the signs comes from the ζ-coefficients [equations (C9)–(C11)], which are antisymmetric functions of ϕ_1 and ϕ_2. Since the coefficients $\zeta^{(1,2,3)}$ govern the rotations of P- and S-wave NMO ellipses in monoclinic media (Grechka et al., 1999), our result indicates that measuring the whole ellipses, not just their semi-axes, is important for estimating the fracture parameters.

Although the resulting approximations (C1)–(C11) may look somewhat complicated, they do allow us to estimate all fracture parameters following, for instance, the strategy explained in Appendix D. To check the accuracy of the derived expressions, we computed the exact anisotropic coefficients for fracture parameters given in Table 1 and carried out the inversion using the linearized expressions from Appendix D. Even though the crack densities for the two systems of fractures $e_1 \approx \Delta_{T1}/2 = 0.06$ and $e_2 \approx \Delta_{T2}/2 = 0.10$ are not that small, Table 1 shows that the derived approximations are sufficiently accurate and, therefore, can be used, at least, for obtaining initial guesses in nonlinear inversion.

Special case: equal tangential weaknesses

It is useful to examine the special case of equal tangential weaknesses of two the systems:

$$\Delta_{T1} = \Delta_{T2} \equiv \Delta_T \,. \tag{10}$$

In this case, equation (9) indicates that

$$\phi_1 = -\phi_2 \equiv \phi \,, \tag{11}$$

i.e., the S-wave polarization directions bisect the angles between the fracture sets (see Figure 2 for $K_{T1}/K_{T2} = 1$). Substituting relations (10) and (11) into equations (C1)–(C11), we derive equations (E3)–(E13) which are easier to invert for the fracture parameters than those for $\Delta_{T1} \neq \Delta_{T2}$. Equations from Appendix E indicate that the fracture azimuth ϕ and the weaknesses Δ_T, Δ_{N1}, and Δ_{N2} can be found from the vertical velocities of P- and shear-waves and the P-wave NMO ellipse; S-wave NMO ellipses provide redundant information.

Approximations from Appendix E allow one to find simple relations between the orientations of the pure-mode NMO ellipses and the azimuths of fractures. For instance, the azimuth θ_P of the semi-major axis of P-wave NMO ellipse can be written in the weak-anisotropy approximation as (Grechka et al., 1999)

$$\tan 2\theta_P = \frac{2\,\zeta^{(3)}}{\delta^{(2)} - \delta^{(1)}}. \tag{12}$$

Substituting equations (E7), (E8), and (E13) into equation (12) yields

$$\tan 2\theta_P = A_P \tan 2\phi \,, \tag{13}$$

where

$$A_P = \frac{(\Delta_{N2} - \Delta_{N1})(1-2g)}{(\Delta_{N1} + \Delta_{N2})(1-2g) + 2\Delta_T} \,. \tag{14}$$

Note that $|A_P| \leq 1$, which means that always $\theta_P \leq \phi$. Therefore, the semi-major axis of the ellipse always lies between the strikes of two fracture sets where the angle between them is less than 90°. This is illustrated in Figure 3 which shows the exact P-wave NMO ellipse (solid) computed for the monoclinic model containing two fracture systems with equal tangential weaknesses. The ellipse semi-major axis points between the fracture strikes (dashed lines) as predicted by equations (13) and (14). The approximation (12) gives an accurate estimate of the azimuth $\theta_P = 8.1°$ compared to its exact value $\theta_P = 6.7°$.

The semi-axes of the P-wave NMO ellipse point along the fracture strikes in the special case of orthogonal fractures for which $2\phi = 90°$, and the effective medium becomes orthorhombic. Another special case of orthorhombic symmetry is that of two identical fracture systems [i.e., $\Delta_{N1} = \Delta_{N2}$ in addition to equation (10)], and all ζ-coefficients given by equations (E11)–(E13) vanish.

Equation (13) indicates that, since $\theta_P \neq 0$, the azimuths of the semi-axes of the P-wave NMO ellipse do

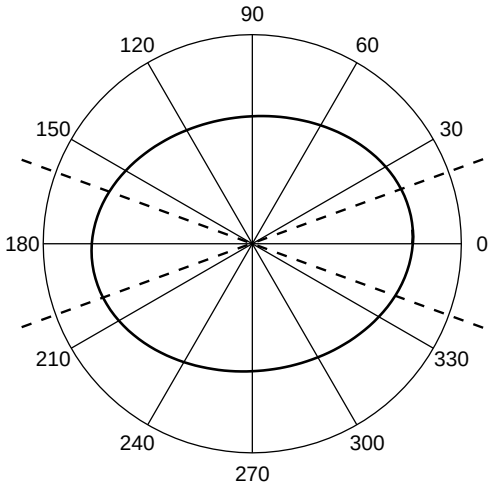

Figure 3. P-wave NMO ellipse from a horizontal reflector in the monoclinic medium produced by two sets of fractures with the weaknesses $\Delta_{N1} = 0$, $\Delta_{N2} = 0.5$, and $\Delta_{T1} = \Delta_{T2} = 0.4$. The angle between the fracture strikes (dashed lines) is $2\phi = 40°$. The squared velocity ratio in the isotropic background is $g = V_S^2/V_P^2 = 1/9$. The azimuths 0° and 90° correspond to the polarization directions of vertically propagating S_1- and S_2-waves.

not coincide with the polarization directions of vertically propagating shear waves, as was noted by Grechka et al. (1999), also, see Sayers (1998). [The same is also true for S_1- and S_2-wave NMO ellipses because their rotations are determined by $\zeta^{(1)}$ and $\zeta^{(2)}$ (Grechka et al. 1999), and $\zeta^{(1)} \neq 0$ and $\zeta^{(2)} \neq 0$, as follows from equations (E11) and (E12).] This may explain the discrepancies in fracture orientation estimated from the P-wave NMO ellipse and S-wave polarizations such as those described by Perez et al. (1999).

Arbitrary fracture sets

Although the linearized approximations for the fracture parameters gave us some insights into the behavior of anisotropic coefficients due to the presence of fractures, here we perform actual inversion based on the exact equations (1)–(4). We assume that the quantities V_{P0}, V_{S0}, $\epsilon^{(1,2)}$, $\delta^{(1,2)}$, $\gamma^{(1,2)}$, and $\zeta^{(1,2,3)}$ have already been estimated from the vertical and moveout velocities of P- and S-waves and introduce errors in all quantities [similar to those shown in Figure 2 and Figure 4 in Grechka et al. (1999)] caused by Gaussian noise with a variance of 2% added to the NMO velocities. The variances of errors in anisotropic parameters are: 2% in V_{P0} and V_{S0}, 0.01 in $\zeta^{(1)}$ and $\zeta^{(2)}$, and 0.03 in all other anisotropic coefficients. We obtain the fracture parameters (using the simplex method) that give the best fit to error-contaminated vertical velocities and anisotropic coefficients.

Figure 4 presents our inversion results for the V_P/V_S ratio in the isotropic background and the weaknesses

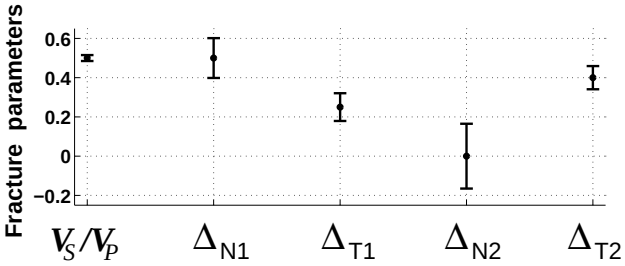

Figure 4. Inversion for the parameters of two crack systems. Dots represent the exact values of the fracture parameters. Bars correspond to ± one standard deviation in the inverted quantities. The standard deviations in the estimated background velocities V_P and V_S (not shown here) are 2.0% and 2.5% accordingly. The standard deviations in the fracture azimuths ϕ_1 and ϕ_2 are 9° (their correct values are $\phi_1 = 30°$ and $\phi_2 = -12.8°$).

Δ_{Ni} and Δ_{Ti}. The standard deviation in the estimated V_P/V_S ratio is 3.1%, which is somewhat higher than the standard deviation of the input vertical velocities V_{P0} and V_{S0}. Error amplification by a factor of about 2 (compared to the errors in the input anisotropic coefficients) is seen for the weaknesses Δ_{Ti}. This can be understood from the weak anisotropy approximations (D6) and (D8), which indicate that Δ_{Ti} are derived from the γ-coefficients [similar results were obtained for models with one system of fractures in Paper I and Paper II]. Those γ-coefficients are multiplied by 2 [equation (D6)] which explains the size of error bars for Δ_{Ti} in Figure 4. The accuracy of the inverted normal weaknesses Δ_{Ni} is even lower than that of Δ_{Ti}. We can explain this, again, using the weak anisotropy approximations (C1)–(C11). Note that all terms in the form $\Delta_{Ti} \pm a\,\Delta_{Ni}$ contain the factors $a < 1$. Therefore, greater variations in Δ_{Ni} than those in Δ_{Ti} are required to compensate for the errors in input anisotropic coefficients. Even though the errors in estimated Δ_{Ni} are relatively large, Figure 4 shows that we can distinguish between dry cracks (the first system of fractures where $K_{N1} \approx K_{T1}$ or $\Delta_{T1}\,(1-\Delta_{N1}) \approx g\,\Delta_{N1}(1-\Delta_{T1})$ within the given error bars) and fluid-filled ones where $\Delta_{N2} \approx 0$. The nonphysical values $\Delta_{N2} < 0$ appear in Figure 4 because random errors added to the data sometimes produce anisotropic coefficients which do not correspond to any fractured media.

Fractures with micro-corrugated faces and fluid-dependent shear-wave splitting

It has been accepted for years that the so called shear-wave splitting parameter $\gamma^{(S)}$ in media with vertical fractures, expressed in terms of the velocities V_{S1} and V_{S2} of vertically propagating shear waves as

$$\gamma^{(S)} \equiv \frac{V_{S1}^2 - V_{S2}^2}{2\,V_{S2}^2}\,, \tag{15}$$

depends only on the crack density and does not contain any information about the fluid content of fractures. This statement seems to be confirmed both experimentally (e.g., Martin and Davis, 1987; Winterstein and Meadows, 1991) and theoretically (e.g., Hudson, 1981). On the other hand, the recent results of Guest et al. (1998), who presented a case study where the shear-wave splitting for gas-filled cracks was significantly higher than that for brine-filled ones, clearly, contradict the existing understanding. Here, we present a possible theoretical explanation of the observations made by Guest et al. (1998). The idea of the theory described below is to couple tangential slips along fracture faces, which determine shear-wave splitting, to the normal slip that is known to depend on fluid content.

Linear slip model for fractures with micro-corrugated faces

We again apply formalism of the linear slip theory developed by Schoenberg (1980), Schoenberg and Muir (1989), and Schoenberg and Sayers (1995). For simplicity, we examine anisotropy produced by one system of parallel fractures with the normal $\mathbf{n} = [1, 0, 0]$ embedded in an isotropic host rock. The matrix of the excess fracture compliance in this case has the form (Schoenberg and Douma, 1988; Paper I)

$$\mathbf{s}_f = \begin{pmatrix} K_N & 0 & 0 & 0 & K_{NV} & K_{NH} \\ 0 & 0 & 0 & 0 & 0 & 0 \\ 0 & 0 & 0 & 0 & 0 & 0 \\ 0 & 0 & 0 & 0 & 0 & 0 \\ K_{NV} & 0 & 0 & 0 & K_V & K_{VH} \\ K_{NH} & 0 & 0 & 0 & K_{VH} & K_H \end{pmatrix}, \qquad (16)$$

where K_N is the normal fracture compliance relating the jump of the displacement normal to the fracture (i.e., the normal slip) to the normal stress in the direction $[1, 0, 0]$. K_V and K_H are the tangential compliances which relate the slips and stresses in the vertical $[0, 0, 1]$ and horizontal $[0, 1, 0]$ directions. The compliance K_{NV} couples the normal slip to tangential vertical stress or, equivalently, the tangential slip in direction $[0, 0, 1]$ to the normal stress. Similarly, the compliances K_{NH} and K_{VH} couple the horizontal stress in the $[0, 1, 0]$ direction to the normal and vertical slips.

The conventional conclusion about the independence of the shear-wave splitting coefficient $\gamma^{(S)}$ from fracture infill is based on the *assumption* that the normal and tangential slips are decoupled ($K_{NV} = K_{NH} = K_{VH} = 0$) and the matrix (16) is diagonal. An alternative model of cracks with micro-corrugated faces was suggested by Schoenberg and Douma (1988). The simplest model of this kind is shown in Figure 5. Since the stresses in either the normal (x_1) or vertical (x_3) direction applied to such a fracture produce slips in both x_1 and x_3 directions, the compliance component K_{NV} has to be nonzero. In contrast, the component K_{VH} can be always set to zero by the appropriate rotation of the coordinate system (Berg et al., 1991). Below, we show that fractures characterized by the compliances

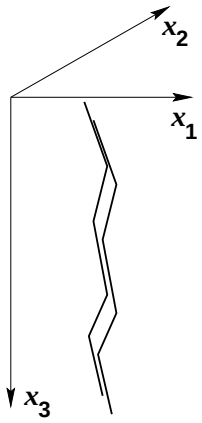

Figure 5. Vertical fracture with microstructure that couples the normal and tangential slips (after Schoenberg and Douma, 1988).

$$K_{NH} = K_{VH} = 0 \quad \text{and} \quad K_{NV} \neq 0\,, \qquad (17)$$

cause infill-dependent shear-wave splitting.

Effective model of fractured media

If a fracture system with the compliances described by equations (16) and (17) is embedded in an isotropic rock, the effective stiffness matrix has the form [see equation (1)]

$$\mathbf{c}^{-1} = \mathbf{s}_b + \mathbf{s}_f\,, \qquad (18)$$

where the background compliance matrix $\mathbf{s}_b$ is given by equation (2).

Evaluating the components of the matrix $\mathbf{c}$ yields

$$\mathbf{c} = \begin{pmatrix} c_{11} & c_{12} & c_{12} & 0 & c_{15} & 0 \\ c_{12} & c_{33} & c_{23} & 0 & c_{35} & 0 \\ c_{12} & c_{23} & c_{33} & 0 & c_{35} & 0 \\ 0 & 0 & 0 & c_{44} & 0 & 0 \\ c_{15} & c_{35} & c_{35} & 0 & c_{55} & 0 \\ 0 & 0 & 0 & 0 & 0 & c_{66} \end{pmatrix}, \qquad (19)$$

i.e., fractures characterized by compliances (16) and (17) produce an effective monoclinic medium with the vertical symmetry plane $[x_1, x_3]$. The elements of the matrix (19) are given by

$$c_{11} = (\lambda + 2\mu)\,\frac{1 + E_V}{D}\,,$$

$$c_{12} = \lambda\,\frac{1 + E_V}{D}\,,$$

$$c_{15} = -\sqrt{\mu(\lambda + 2\mu)}\,\frac{E_{NV}}{D}\,,$$

$$c_{33} = (\lambda + 2\mu)\,\frac{(1+E_V)(1+\nu E_N) - \nu E_{NV}^2}{D}\,,$$

$$c_{23} = \lambda\,\frac{(1+2gE_N)(1+E_V) - 2gE_{NV}^2}{D}\,,$$

$$c_{35} = -\lambda\,\frac{\sqrt{g}E_{NV}}{D}\,,$$

$$c_{44} = \mu\,,$$

$$c_{55} = \mu\,\frac{1+E_N}{D}\,,$$

and

$$c_{66} = \frac{\mu}{1+E_H}\,,$$

where

$$D = (1+E_N)(1+E_V) - E_{NV}^2\,,$$

$$\nu = \frac{4\mu(\lambda+\mu)}{(\lambda+2\mu)^2}\,,$$

$$g = \frac{\mu}{\lambda+2\mu}\,;$$

λ and μ are the Lamé constants of the host rock. The dimensionless compliances E_N, E_V, E_H, and E_{NV} are defined as follows (Hsu and Schoenberg, 1993):

$$E_N = (\lambda+2\mu)K_N\,, \tag{20}$$

$$E_V = \mu K_V\,, \tag{21}$$

$$E_H = \mu K_H\,, \tag{22}$$

and

$$E_{NV} = \sqrt{\mu(\lambda+2\mu)}K_{NV}\,. \tag{23}$$

The stability condition requires that the matrix (16) be nonnegative definite. In our case, this condition implies that all dimensionless compliances E_N, E_V, and E_H are nonnegative, and

$$E_N E_V - E_{NV}^2 \geq 0\,. \tag{24}$$

Shear-wave splitting coefficient

The split shear waves traveling in the vertical direction in the monoclinic medium (19) have the velocities V_{S1} and V_{S2} given by

$$V_{S1}^2 = \frac{\mu}{\rho}\,, \tag{25}$$

and

$$V_{S2}^2 = \frac{2}{\rho}\,\frac{c_{33}\,c_{55} - c_{35}^2}{c_{33} + c_{55} + \sqrt{(c_{33}-c_{55})^2 + 4\,c_{35}^2}}\,, \tag{26}$$

where ρ is the density. While the velocity V_{S1} of the fast shear wave is independent of fractures and equal to the background S-wave velocity, the velocity V_{S2} does depend on the fracture compliances E_N, E_T, and E_{NV}.

Assuming weak anisotropy, i.e., $E_N \ll 1$, $E_T \ll 1$, and $E_{NV} \ll 1$, and keeping the terms up to quadratic in dimensionless compliances, we obtain an approximate shear-wave splitting coefficient [equation (15)] as

$$\gamma^{(S)} \approx \frac{E_V}{2} - \frac{E_{NV}^2\,g\,(3-4\,g)}{2\,(1-g)}\,, \tag{27}$$

which shows that the coupling between the normal and tangential slips always *reduces* the value of $\gamma^{(S)}$.

To analyze the influence of fluid content on shear-wave splitting for fractures with micro-corrugated faces, we generalize the criteria given by Schoenberg and Sayers (1995), who pointed out that $K_N/K_V = 0$ for fluid-saturated isolated penny-shaped cracks and $K_N/K_V = 1$ for dry ones. The result of Schoenberg and Sayers (1995) is formulated for $K_{NV} = 0$. Let us consider the 2×2 submatrix

$$\tilde{\mathbf{s}}_f = \begin{pmatrix} K_N & K_{NV} \\ K_{NV} & K_V \end{pmatrix} \tag{28}$$

of the compliance matrix (16) and note that the Schoenberg-Sayers criteria for $K_{NV} = 0$ are equivalent to the statements that the fractures are dry if the matrix $\tilde{\mathbf{s}}_f$ has two equal eigenvalues, and the fractures are fluid-filled if one eigenvalue of $\tilde{\mathbf{s}}_f$ is zero. We *assume* that the same relationship between fluid saturation of the fractures and eigenvalues of the matrix $\tilde{\mathbf{s}}_f$ also holds when $K_{NV} \neq 0$. To justify this assumption, we remind the main concept of the linear slip theory that the excess compliance matrix $\mathbf{s}_f$ relates the stress applied to the fracture faces to the jump of the displacement (i.e., the slip) across the fractures (Schoenberg, 1980). The eigenvalues of the matrices $\mathbf{s}_f$ or $\tilde{\mathbf{s}}_f$ are simply the coefficients that relate the magnitudes of the slip and the stress vectors in the principal directions, where those vectors are parallel to each other. Intuitively, it is clear that dry fractures are equally compliant in all directions (there is no material inside to stiffen them) and all eigenvalues of the fracture compliance matrix are supposed to be equal. In contrast, fluid-filled fractures are noticeably stiffer in a particular direction where the applied stress tends to squeeze the fluid. Thus, the eigenvalue corresponding to this direction is expected to be significantly smaller than the other eigenvalues.

The matrix (28) has equal eigenvalues if and only if $K_N = K_V$ and $K_{NV} = 0$ which means [see equation (23)] that

$$E_{NV} = 0\,. \tag{29}$$

The presence of zero eigenvalue of $\tilde{\mathbf{s}}_f$ requires that $K_{NV}^2 = K_N K_V$ or [equations (20)–(23)]

$$E_{NV}^2 = E_N E_V\,. \tag{30}$$

Since $E_{NV}^2 \leq E_N E_V$ [inequality (24)], equations (29)

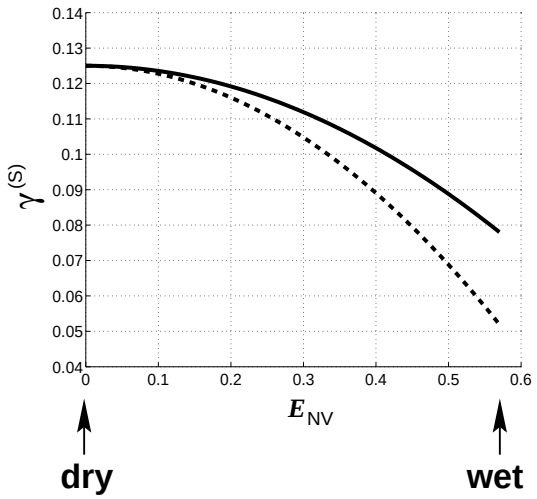

Figure 6. Shear-wave splitting coefficient $\gamma^{(S)}$ computed using the exact equations (15), (25), and (26) (solid) and the approximation (27) (dashed) as a function of the dimensionless compliance E_{NV}. The model parameters are $g = 0.16$, $E_N = 1.3$, and $E_V = 0.25$.

and (30) put strict bounds on possible absolute values of E_{NV}.

Substituting equations (29) and (30) into formula (27) yields the shear-wave splitting coefficients for dry and fluid-filled cracks:

$$\gamma^{(S)}_{dry} \approx \frac{E_V}{2} \tag{31}$$

and

$$\gamma^{(S)}_{wet} \approx \frac{E_V}{2}\left[1 - \frac{E_N\, g\,(3-4\,g)}{1-g}\right]. \tag{32}$$

We observe that always $\gamma^{(S)}_{dry} \geq \gamma^{(S)}_{wet}$, which is consistent with the observations of Guest et al. (1998). Figure 6 illustrates the influence of the dimensionless compliance E_{NV} on the shear-wave splitting coefficient that decreases by about 30% as gas is replaced with a fluid. Also note that approximation (27) gives a reasonable accurate estimate of $\gamma^{(S)}$.

Discussion and conclusions

This paper completes our series of three papers (see also Paper I and Paper II) where we examine the feasibility of estimating fracture parameters using anisotropic coefficients determined from various seismic signatures. We began Paper I by showing that the fracture compliances or dimensionless fracture weaknesses are the only quantities which can be unambiguously estimated from seismic data, whereas obtaining information about fracture microstructure (such as the shape of cracks, their possible interaction, the presence of equant porosity, etc.) is generally beyond the capabilities of seismic method. If the fractures are penny-shaped, however, the weaknesses give direct estimates of the crack density and fluid content of the fractures. Then, we discussed the inversion for the compliances of fractures that produce effective HTI and orthorhombic media (Paper I and Paper II). Finally, in this paper we estimated parameters of two non-orthogonal sets of rotationally invariant fractures which lead to effective media of monoclinic symmetry.

We have demonstrated that the weaknesses and azimuths of two non-orthogonal fracture systems can be obtained using the vertical velocities of P- and two split shear-waves and their NMO ellipses corresponding to reflections from horizontal interfaces. Estimation of fracture parameters was performed in the natural coordinate frame which horizontal axes coincide with polarization directions of vertically propagating S-waves. Those directions are governed by the weaknesses Δ_{Ti} tangential to the fracture faces and are independent from the normal weaknesses Δ_{Ni}. In the case of equal tangential weaknesses $\Delta_{T1} = \Delta_{T2}$, shear-wave polarization directions bisect the angles between two fracture systems, and all fracture weaknesses can be obtained from the shear-wave splitting coefficient $\gamma^{(S)}$ and the P-wave NMO ellipse. It is important to note that the azimuths of the semi-axes of the P-wave NMO ellipse generally deviate from the polarization directions of shear waves (the same is true for S-wave NMO ellipses). This result may explain some existing experimental observations (e.g., Perez et al., 1999) that the so-called "predominant" fracture orientation obtained by P-wave azimuthal moveout analysis differs from that estimated from shear-wave polarization directions.

We have also examined the model which contains one system of vertical fractures with micro-corrugated surfaces in an isotropic background. An important feature of this model is the coupling of slips in the directions normal and tangential to crack faces. Such a coupling makes it possible to explain the dependence of the shear-wave splitting coefficient $\gamma^{(S)}$ (which is determined by the tangential slip or tangential weakness) on the fluid content of the fractures (which influences the normal slip). We showed that $\gamma^{(S)}$ may noticeable vary with fluid saturation. Although it is conventionally believed that the shear-wave splitting is independent of fluid content, our model is consistent with the recent observations of Guest et al. (1998).

Acknowledgments

This work has been done during visit of Andrey Bakulin to the Center for Wave Phenomena (CWP), Colorado School of Mines. We thank Sean Guest and Cees van der Kolk of Shell for their provocative discussion of the shear-wave splitting coefficient. We are also grateful to members of the A(nisotropy)-team of CWP for help-

ful discussions. The support for this work was provided by the members of the Consortium Project on Seismic Inverse Methods for Complex Structures at CWP and by the United States Department of Energy (project "Three-Dimensional Analysis of Seismic Signatures and Characterization of Fluids and Fractures in Anisotropic Formations", award #DE-FG03-98ER14908).

References

Bakulin, A.V, Grechka, V., and Tsvankin, I., 1999a, (Paper I) Estimation of fracture parameters from reflection seismic data. Part I: HTI model due to a single fracture set: this volume.

Bakulin, A.V, Grechka, V., and Tsvankin, I., 1999b, (Paper II) Estimation of fracture parameters from reflection seismic data. Part II: Fractured models with orthorhombic symmetry: this volume.

Bakulin, A.V, and Molotkov, L.A., 1998, Effective models of fractured and porous media: St.Petersburg University Press (in Russian).

Berg, E., Hood, J.A., and Fryer, G.J., 1991, Reduction of the general fracture compliance matrix **Z** to only five independent elements: Geophys. J. Int., **107**, 703–707.

Grechka, V., Contreras, P., and Tsvankin, I., 1999, Inversion of normal moveout for monoclinic media: this volume.

Grechka, V., and Tsvankin, I., 1998, 3-D description of normal moveout in anisotropic media: Geophysics, **63**, 1079–1092.

Grechka, V., and Tsvankin, I., 1999, Moveout velocity analysis and parameter estimation in orthorhombic media: Geophysics, in print.

Guest, S., van der Kolk, C., Potters, H., 1998, The effect of fracture filling fluids on shear-wave propagation: 68th Ann. Internat. Mtg., Soc. Expl. Geophys., Expanded Abstracts, 948–951.

Helbig, K., 1994, Foundations of anisotropy for exploration seismics, in Handbook of Geophysical Exploration, **22**, eds Helbig, K. and Treitel, S.: Pergamon Press.

Hsu, C.-J., and Schoenberg, M., 1993, Elastic waves through a simulated fractured medium: Geophysics, **58**, 964–977.

Hudson, J.A., 1980, Overall properties of a cracked solid: Math. Proc. Camb. Phil. Soc., **88**, 371–384.

Hudson, J.A., 1981, Wave speeds and attenuation of elastic waves in material containing cracks: Geophys. J. Roy. Astr. Soc., **64**, 133–150.

Hudson, J.A., 1988, Seismic wave propagation through material containing partially saturated cracks: Geophys. J., **92**, 33–37.

Martin, M.A., and Davis, T.L., 1987, Shear-wave birefringence: A new tool for evaluating fractured reservoirs: The Leading Edge, **6**, 22–28.

Mensch, T., and Rasolofosaon, P., 1997, Elastic-wave velocities in anisotropic media of arbitrary symmetry – generalization of Thomsen's parameters ϵ, δ, and γ: Geophys. J. Int., **128**, 43–64.

Molotkov, L.A., and Bakulin, A.V., 1997, An effective model of a fractured medium with fractures modeled by the surfaces of discontinuity of displacements: Journal of Mathematical Sciences, **86**, N 3, 2735–2746

Nichols, D., Muir, F., and Schoenberg, M., 1989, Elastic properties of rocks with multiple sets of fractures: 59th Ann. Internat. Mtg., Soc. Expl. Geophys., Expanded Abstracts, 471–474.

Perez, M.A., Grechka, V., and Michelena, R.J., 1999, Fracture detection in a carbonate reservoir using a variety of seismic methods: Geophysics, in print.

Rüger, A., 1997, P-wave reflection coefficients for transversely isotropic models with vertical and horizontal axis of symmetry: Geophysics, **62**, 713–722.

Sayers, C., 1998, Misalignment of the orientation of fractures and the principal axes for P and S waves in rocks containing multiple non-orthogonal fracture sets: Geophys. J. Int., **133**, 459–466.

Schoenberg, M., 1980, Elastic wave behavior across linear slip interfaces: J. Acoust. Soc. Am., **68**, 1516–1521.

Schoenberg, M., 1983, Reflection of elastic waves from periodically stratified media with interfacial slip: Geophys. Prosp., **31**, 265–292.

Schoenberg, M., Dean, S., and Sayers, C., 1999, Azimuth-dependent tuning of seismic waves reflected from fractured reservoirs: Geophysics, submitted.

Schoenberg, M., and Douma, J., 1988, Elastic wave propagation in media with parallel fractures an aligned cracks: Geophys. Prosp., **36**, 571–590.

Schoenberg, M., and Muir, F., 1989, A calculus for finely layered anisotropic media: Geophysics, **54**, 581–589.

Schoenberg, M., and Sayers, C., 1995, Seismic anisotropy of fractured rock: Geophysics, **60**, 204–211.

Thomsen, L., 1986, Weak elastic anisotropy: Geophysics, **51**, 1954–1966.

Thomsen, L., 1995, Elastic anisotropy due to aligned cracks in porous rock : Geophys. Prosp., **43**, 805–830.

Tsvankin, I., 1997a, Reflection moveout and parameter estimation for horizontal transverse isotropy: Geophysics, **62**, 614 –629.

Tsvankin, I., 1997b, Anisotropic parameters and P-wave velocity for orthorhombic media: Geophysics, **62**, 1292–1309.

Winterstein, D.F., 1990, Velocity anisotropy terminology for geophysicists: Geophysics, **55**, 1070–1088.

Winterstein, D.F., and Meadows, M.A., 1991, Shear-

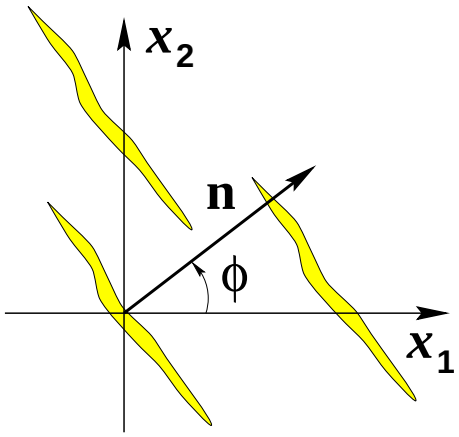

Figure A1. Set of vertical fractures oriented at azimuth ϕ with respect to x_1-axis of selected coordinate frame. The angle ϕ is positive in counter-clockwise direction.

wave polarizations and subsurface stress directions at Lost Hills field: Geophysics, **56**, 1331–1348.

APPENDIX A: Compliance of rotated fracture set

Applying Bond transformation (4) [see Winterstein (1990)] to the fracture compliance matrix (3), Schoenberg et al. (1999) obtained matrix $\mathbf{s}_f$ (for brevity, the number i of fracture set is omitted) which describes compliance of the fracture set with normal $\mathbf{n} = [\cos\phi, \sin\phi, 0]$. (Figure A1). Matrix $\mathbf{s}_f$ has the following nonzero elements:

$$s_{11\,f} = \frac{3\,K_N + K_T}{8} + \frac{K_N}{2}\cos 2\phi + \frac{K_N - K_T}{8}\cos 4\phi\,, \quad \text{(A1)}$$

$$s_{12\,f} = \frac{K_N - K_T}{8}\,(1 - \cos 4\phi)\,, \quad \text{(A2)}$$

$$s_{16\,f} = \frac{K_N}{2}\sin 2\phi + \frac{K_N - K_T}{4}\sin 4\phi\,, \quad \text{(A3)}$$

$$s_{22\,f} = \frac{3\,K_N + K_T}{8} - \frac{K_N}{2}\cos 2\phi + \frac{K_N - K_T}{8}\cos 4\phi\,, \quad \text{(A4)}$$

$$s_{26\,f} = \frac{K_N}{2}\sin 2\phi - \frac{K_N - K_T}{4}\sin 4\phi\,, \quad \text{(A5)}$$

$$s_{44\,f} = K_T\,\frac{1 - \cos 2\phi}{2}\,, \quad \text{(A6)}$$

$$s_{45\,f} = K_T\,\frac{\sin 2\phi}{2}\,, \quad \text{(A7)}$$

$$s_{55\,f} = K_T\,\frac{1 + \cos 2\phi}{2}\,, \quad \text{(A8)}$$

$$s_{66\,f} = \frac{K_N + K_T}{2} - \frac{K_N - K_T}{2}\cos 4\phi\,. \quad \text{(A9)}$$

APPENDIX B: Anisotropic parameters in monoclinic media

Selecting the coordinate frame which horizontal x_1- and x_2-axes coincide with the polarization directions of S_1- and S_2-waves, Grechka et al. (1999) defined anisotropic parameters for media of monoclinic symmetry by analogy with Thomsen's (1986) and Tsvankin's (1997b) parameterizations introduced in VTI and orthorhombic media. Expressions for these parameters in terms of density ρ and elastic stiffness coefficients are given below.

V_{P0} – P-wave vertical velocity:

- $V_{P0} \equiv \sqrt{\dfrac{c_{33}}{\rho}}\,;$ (B1)

V_{S0} – the vertical velocity of S_1-wave polarized in the x_1-direction:

- $V_{S0} \equiv \sqrt{\dfrac{c_{55}}{\rho}}\,;$ (B2)

- $\epsilon^{(1)} \equiv \dfrac{c_{22} - c_{33}}{2\,c_{33}}\,;$ (B3)

- $\delta^{(1)} \equiv \dfrac{(c_{23} + c_{44})^2 - (c_{33} - c_{44})^2}{2\,c_{33}\,(c_{33} - c_{44})}\,;$ (B4)

- $\gamma^{(1)} \equiv \dfrac{c_{66} - c_{55}}{2\,c_{55}}\,;$ (B5)

- $\epsilon^{(2)} \equiv \dfrac{c_{11} - c_{33}}{2\,c_{33}}\,;$ (B6)

- $\delta^{(2)} \equiv \dfrac{(c_{13} + c_{55})^2 - (c_{33} - c_{55})^2}{2\,c_{33}\,(c_{33} - c_{55})}\,;$ (B7)

- $\gamma^{(2)} \equiv \dfrac{c_{66} - c_{44}}{2\,c_{44}}\,;$ (B8)

- $\delta^{(3)} \equiv \dfrac{(c_{12} + c_{66})^2 - (c_{11} - c_{66})^2}{2\,c_{11}\,(c_{11} - c_{66})}\,;$ (B9)

$\zeta^{(1)}$ – the parameter responsible for the rotation of S_1-wave NMO ellipse:

- $\zeta^{(1)} \equiv \dfrac{c_{16} - c_{36}}{2\,c_{33}}\,;$ (B10)

$\zeta^{(2)}$ – the parameter responsible for the rotation of S_2-wave NMO ellipse:

- $\zeta^{(2)} \equiv \dfrac{c_{26} - c_{36}}{2\,c_{33}}\,;$ (B11)

$\zeta^{(3)}$ – the parameter responsible for the rotation of P-wave NMO ellipse:

- $\zeta^{(3)} \equiv \dfrac{c_{36}}{c_{33}}\,.$ (B12)

Parameters (B1)–(B9) exactly correspond to those defined by Tsvankin (1997b) in orthorhombic media. The coefficient $\zeta^{(3)}$ is analogous to the anisotropic parameter

χ_z introduced by Mensch and Rasolofosaon (1997).

APPENDIX C: Parameters of fractured media in the case of weak anisotropy

Here, we use equations (1)–(4) and relations from Appendix A to express anisotropic coefficients (B1)–(B8) and (B10)–(B12) via fracture parameters. We assume that $\Delta_{Ni} \ll 1$ and $\Delta_{Ti} \ll 1$ so that anisotropy of effective medium is weak. Keeping only linear in Δ_{Ni} and Δ_{Ti} terms, we obtain the following expressions:

$$V_{P0} = V_P \left[1 - \frac{(1-2\,g)^2}{2}\,(\Delta_{N1} + \Delta_{N2})\right], \tag{C1}$$

$$V_{S0} = V_S \left[1 - \frac{\Delta_{T1}}{4}\,(1+\cos 2\phi_1) - \frac{\Delta_{T2}}{4}\,(1+\cos 2\phi_2)\right], \tag{C2}$$

$$\epsilon^{(1)} = -2\,g\Big\{\Big[(1-g)\,\Delta_{N1} + (\Delta_{T1} - g\,\Delta_{N1})\cos^2\phi_1\Big]\,\sin^2\phi_1 + \Big[(1-g)\,\Delta_{N2} + (\Delta_{T2} - g\,\Delta_{N2})\cos^2\phi_2\Big]\,\sin^2\phi_2\Big\}, \tag{C3}$$

$$\epsilon^{(2)} = -2\,g\Big\{\Big[(1-g)\,\Delta_{N1} + (\Delta_{T1} - g\,\Delta_{N1})\sin^2\phi_1\Big]\,\cos^2\phi_1 + \Big[(1-g)\,\Delta_{N2} + (\Delta_{T2} - g\,\Delta_{N2})\sin^2\phi_2\Big]\,\cos^2\phi_2\Big\}, \tag{C4}$$

$$\delta^{(1)} = -2\,g\Big\{[(1-2\,g)\,\Delta_{N1} + \Delta_{T1}]\,\sin^2\phi_1 + [(1-2\,g)\,\Delta_{N2} + \Delta_{T2}]\,\sin^2\phi_2\Big\}, \tag{C5}$$

$$\delta^{(2)} = -2\,g\Big\{[(1-2\,g)\,\Delta_{N1} + \Delta_{T1}]\,\cos^2\phi_1 + [(1-2\,g)\,\Delta_{N2} + \Delta_{T2}]\,\cos^2\phi_2\Big\}, \tag{C6}$$

$$\gamma^{(1)} = \left[2\,(\Delta_{T1} - g\,\Delta_{N1})\,\cos^2\phi_1 - \frac{\Delta_{T1}}{2}\right]\,\sin^2\phi_1 + \left[2\,(\Delta_{T2} - g\,\Delta_{N2})\,\cos^2\phi_2 - \frac{\Delta_{T2}}{2}\right]\,\sin^2\phi_2, \tag{C7}$$

$$\gamma^{(2)} = \left[2\,(\Delta_{T1} - g\,\Delta_{N1})\,\sin^2\phi_1 - \frac{\Delta_{T1}}{2}\right]\,\cos^2\phi_1 + \left[2\,(\Delta_{T2} - g\,\Delta_{N2})\,\sin^2\phi_2 - \frac{\Delta_{T2}}{2}\right]\,\cos^2\phi_2, \tag{C8}$$

$$\zeta^{(1)} = \frac{g}{4}\left[2\,g\,(\Delta_{N1}\,\sin 2\phi_1 + \Delta_{N2}\,\sin 2\phi_2) - (\Delta_{T1} - g\,\Delta_{N1})\,\sin 4\phi_1 - (\Delta_{T2} - g\,\Delta_{N2})\,\sin 4\phi_2\right], \tag{C9}$$

$$\zeta^{(2)} = \frac{g}{4}\left[2\,g\,(\Delta_{N1}\,\sin 2\phi_1 + \Delta_{N2}\,\sin 2\phi_2) + (\Delta_{T1} - g\,\Delta_{N1})\,\sin 4\phi_1 + (\Delta_{T2} - g\,\Delta_{N2})\,\sin 4\phi_2\right], \tag{C10}$$

and

$$\zeta^{(3)} = g\,(1-2\,g)\,(\Delta_{N1}\,\sin 2\phi_1 + \Delta_{N2}\,\sin 2\phi_2), \tag{C11}$$

where V_P and V_S are the P- and S-wave velocities in isotropic background, and

$$g = \frac{V_S^2}{V_P^2}. \tag{C12}$$

The derived approximations allow one to obtain two relations which show that anisotropic coefficients are not independent. Combining equations (C9)–(C11), we see that

$$\frac{\zeta^{(3)}}{\zeta^{(1)} + \zeta^{(2)}} = \frac{1}{g} - 2\,. \tag{C13}$$

It can be proven that this result is exact, i.e., valid for any strength of anisotropy.

Another relation, which follows from equations (C3)–(C8),

$$\delta^{(1)} - \delta^{(2)} = 4g(\gamma^{(1)} - \gamma^{(2)}) + \frac{1-2g}{1-g}(\epsilon^{(1)} - \epsilon^{(2)}) \tag{C14}$$

is the same as that derived in Paper II for one system of fractures in VTI host medium.

APPENDIX D: Estimation of fracture parameters in the weak anisotropy limit

The linearized estimates of all fracture parameters can be obtained using approximations (C1)–(C11). This is achieved following the strategy below.

- Three ζ-coefficients combined in the form [equation (C13)]

$$\frac{\zeta^{(3)}}{\zeta^{(1)} + \zeta^{(2)}} = \frac{1}{g} - 2 \tag{D1}$$

give the value of of g or the V_S/V_P ratio [see equation (C12)] in isotropic host medium. Another, probably more robust, option is to estimate g from the ratio of vertical velocities $g = V_{P0}^2/V_{S0}^2$ [see equations (C1) and (C2)].

- Two combinations

$$\delta^{(1)} + \delta^{(2)} = -2\,g\,[(1-2\,g)\,(\Delta_{N1} + \Delta_{N2}) + (\Delta_{T1} + \Delta_{T2})] \tag{D2}$$

and

$$\epsilon^{(1)} + \epsilon^{(2)} + g\,(\gamma^{(1)} + \gamma^{(2)}) = -\frac{g}{2}\,[4\,(1-g)\,(\Delta_{N1} + \Delta_{N2}) + (\Delta_{T1} + \Delta_{T2})] \tag{D3}$$

allow us to find the sums

$$\Delta_{N1} + \Delta_{N2} = \frac{A - B}{3 - 2\,g} \equiv \mathcal{S}_{\Delta_N} \tag{D4}$$

and

$$\Delta_{T1} + \Delta_{T2} = \frac{4\,(g-1)\,A + (1-2\,g)\,B}{3-2\,g} \equiv \mathcal{S}_{\Delta_T}\,, \tag{D5}$$

where

$$A = \frac{\delta^{(1)} + \delta^{(2)}}{2\,g}$$

and

$$B = \frac{2}{g}\,\left[\epsilon^{(1)} + \epsilon^{(2)} + g\,(\gamma^{(1)} + \gamma^{(2)})\right]\,.$$

- Equations (C7) and (C8), rewritten in the form

$$\Delta_{T1}\cos 2\phi_1 + \Delta_{T2}\cos 2\phi_2 = 2\,(\gamma^{(1)} - \gamma^{(2)}) \equiv \mathcal{D}_\gamma\,, \tag{D6}$$

along with the linearized equation (9)

$$\Delta_{T1}\sin 2\phi_1 + \Delta_{T2}\sin 2\phi_2 = 0 \tag{D7}$$

and equation (D5) can be solved for Δ_{T1} and Δ_{T2} which gives

$$\Delta_{T1} = \frac{\mathcal{D}_\gamma \sin 2\phi_2}{\sin 2(\phi_2 - \phi_1)}\,, \quad \Delta_{T2} = \frac{-\mathcal{D}_\gamma \sin 2\phi_1}{\sin 2(\phi_2 - \phi_1)}\,, \tag{D8}$$

and

$$\mathcal{D}_\gamma \cos(\phi_2 + \phi_1) = \mathcal{S}_{\Delta_T}\cos(\phi_2 - \phi_1)\,. \tag{D9}$$

Note that the denominators in equations (D8) do not vanish when Δ_{T1} goes to Δ_{T2} because the azimuths ϕ_1 and ϕ_2 have opposite signs so that $\phi_1 \to -\phi_2$ in this case.

- Similarly, making the following combinations of equations (C3), (C4), (C9), (C10)

$$\Delta_{N1}\cos 2\phi_1 + \Delta_{N2}\cos 2\phi_2 = \frac{\epsilon^{(1)} - \epsilon^{(2)}}{2\,g\,(1-g)} \equiv \mathcal{D}_\epsilon \tag{D10}$$

and

$$\Delta_{N1}\sin 2\phi_1 + \Delta_{N2}\sin 2\phi_2 = \frac{\zeta^{(2)} + \zeta^{(1)}}{g^2} \equiv \mathcal{S}_\zeta\,, \tag{D11}$$

and using equation (D4) yields the relations

$$\Delta_{N1} = \frac{\mathcal{D}_\epsilon \sin 2\phi_2 - \mathcal{S}_\zeta \cos 2\phi_2}{\sin 2(\phi_2 - \phi_1)}\,, \tag{D12}$$

$$\Delta_{N2} = \frac{-\mathcal{D}_\epsilon \sin 2\phi_1 + \mathcal{S}_\zeta \cos 2\phi_1}{\sin 2(\phi_2 - \phi_1)}\,, \tag{D13}$$

and

$$\mathcal{D}_\epsilon \cos(\phi_2 + \phi_1) + \mathcal{S}_\zeta \sin(\phi_2 + \phi_1) = \mathcal{S}_{\Delta_N}\cos(\phi_2 - \phi_1)\,. \tag{D14}$$

- Equations (D9) and (D14) can be solved to produce

$$\phi_2 + \phi_1 = \arctan\,\frac{\mathcal{D}_\gamma \mathcal{S}_{\Delta_N} - \mathcal{D}_\epsilon \mathcal{S}_{\Delta_T}}{\mathcal{S}_{\Delta_T}\mathcal{S}_\zeta}\,, \tag{D15}$$

then, equation (D9) yields

$$\phi_2 - \phi_1 = \arccos\,\left[\frac{\mathcal{D}_\gamma}{\mathcal{S}_{\Delta_T}}\cos(\phi_2 + \phi_1)\right]\,. \tag{D16}$$

- Equations (D15) and (D16) allow obtaining the azimuths ϕ_1 and ϕ_1. Then, the weaknesses Δ_{Ti} and Δ_{Ni} are found from equations (D8), (D12), and (D13). Finally, P- and S-wave velocities in the background can be calculated from equations (C1) and (C2).

APPENDIX E: Anisotropic and fracture parameters in the case of equal tangential weaknesses

Here, we assume that tangential weaknesses of both crack systems are equal, i.e.,

$$\Delta_{T1} = \Delta_{T2} \equiv \Delta_T\,. \tag{E1}$$

In this case, equation (9) gives

$$\phi_1 = -\phi_2 \equiv \phi\,. \tag{E2}$$

Substituting those relations into equations (C1)–(C11) yields

$$V_{P0} = V_P\,\left[1 - \frac{(1-2\,g)^2}{2}\,(\Delta_{N1} + \Delta_{N2})\right]\,, \tag{E3}$$

$$V_{S0} = V_S\,\left[1 - \frac{\Delta_T}{2}\,(1 + \cos 2\phi)\right]\,, \tag{E4}$$

$$\epsilon^{(1)} = -2g\big\{(1-g)(\Delta_{N1} + \Delta_{N2}) + [2\Delta_T - g(\Delta_{N1} + \Delta_{N2})]\cos^2\phi\big\}\sin^2\phi\,, \tag{E5}$$

$$\epsilon^{(2)} = -2g\big\{(1-g)(\Delta_{N1} + \Delta_{N2}) + [2\Delta_T - g(\Delta_{N1} + \Delta_{N2})]\sin^2\phi\big\}\cos^2\phi\,, \tag{E6}$$

$$\delta^{(1)} = -2g\,\{(1-2\,g)(\Delta_{N1} + \Delta_{N2}) + 2\,\Delta_T\}\sin^2\phi\,, \tag{E7}$$

$$\delta^{(2)} = -2g\,\{(1-2\,g)(\Delta_{N1} + \Delta_{N2}) + 2\,\Delta_T\}\cos^2\phi\,, \tag{E8}$$

$$\gamma^{(1)} = \big\{2\,[2\Delta_T - g\,(\Delta_{N1} + \Delta_{N2})]\,\cos^2\phi - \Delta_T\big\}\sin^2\phi\,, \tag{E9}$$

$$\gamma^{(2)} = \big\{2\,[2\Delta_T - g\,(\Delta_{N1} + \Delta_{N2})]\,\sin^2\phi - \Delta_T\big\}\cos^2\phi\,, \tag{E10}$$

$$\zeta^{(1)} = 2\,g^2\,(\Delta_{N1} - \Delta_{N2})\sin\phi\cos^3\phi\,, \tag{E11}$$

$$\zeta^{(2)} = 2\,g^2\,(\Delta_{N1} - \Delta_{N2})\sin^3\phi\cos\phi\,, \tag{E12}$$

$$\zeta^{(3)} = g\,(1-2\,g)(\Delta_{N1} - \Delta_{N2})\sin 2\phi\,. \tag{E13}$$

Equations (E3)–(E13) are not difficult to invert for the fracture parameters. Having estimated g from either equation (D1) or V_{S0}/V_{P0} ratio, we can use any of the ratios

$$\frac{\delta^{(1)}}{\delta^{(2)}} = \frac{\zeta^{(2)}}{\zeta^{(1)}} = \tan^2\phi \tag{E14}$$

to find the fracture azimuth ϕ. The angle between two systems of cracks is $2\,\phi$. Knowing ϕ, we can obtain the tangential weakness Δ_T from the shear-wave splitting coefficient $\gamma^{(S)}$ which, in the weak anisotropy limit, equals to the difference between $\gamma^{(2)}$ and $\gamma^{(1)}$:

$$\gamma^{(S)} = \gamma^{(2)} - \gamma^{(1)} = -\Delta_T \cos 2\phi\,. \tag{E15}$$

Then, either of equations (E11)–(E13) for ζ-coefficients gives the difference of the normal weaknesses $\Delta_{N1} - \Delta_{N2}$. There are several ways of obtaining the sum $\Delta_{N1} + \Delta_{N2}$. It can be found, for instance, from the sum of two δ-coefficients [equations (E7) and (E8)]:

$$\Delta_{N1} + \Delta_{N2} = \frac{1}{2\,g - 1}\left(\frac{\delta^{(1)} + \delta^{(2)}}{2\,g} + 2\,\Delta_T\right), \tag{E16}$$

which, together with the difference $\Delta_{N1} - \Delta_{N2}$, yields both normal weaknesses Δ_{N1} and Δ_{N2} individually.